

EXCHANGE INTERACTIONS AND SPIN NONCOLLINEARITY IN HEXAGONAL FERRITES

M. P. PETROV and A. V. KUNEVICH

Physico-technical Institute, USSR Academy of Sciences

Submitted June 21, 1972

Zh. Eksp. Teor. Fiz. 63, 2239-2247 (December, 1972)

The hexagonal ferrites $MFe_{12}O_{19}$ ($M = Ba, Sr, Pb$) and $BaMeFe_{16}O_{27}$ ($Me = Ni, Mg$) are studied by the nuclear magnetic resonance technique. Data on NMR spectra, temperature dependences of sublattice magnetization and parameters of the major exchange interactions are obtained. For the first time data are obtained which indicate that the sublattice magnetic moments may deviate from an antiparallel arrangement in the $BaFe_{12}O_{19}$ single crystal.

HEXAGONAL ferrites are used successfully as microwave materials, owing to the narrow widths of the ferromagnetic-resonance lines in the millimeter band, and to the high electric resistivity and the large values of the anisotropy fields. Most materials are synthesized on the basis of uniaxial hexagonal ferrites with structure $MFe_{12}O_{19}$, where $M = Ba, Sr, or Pb$. It is therefore particularly important to study in detail the properties of just these ferrites. Important information on the temperature dependences of the sublattice magnetization, the relative arrangement of the magnetic moments, the values of the exchange integrals, the cation distribution, and the relaxation processes can be obtained by using the nuclear magnetic resonance (NMR) method. Generally speaking, data on the temperature dependence of local magnetic fields and magnetizations of the sublattice, can be obtained by using the Mossbauer-effect method^[1-6]. However, owing to the small resolution of the method itself and the complicated structure of the hexagonal ferrites, (the presence of five non-equivalent positions of the Fe^{+3} ions), there are certain inaccuracies both in the identification and in the determination of the values of the local fields^[1,2,7].

We present here the results of an NMR investigation of hexagonal ferrites with structure M or W . The first investigations of NMR in $MFe_{12}O_{16}$, with $M = Ba$, were performed by Streever^[8] and by the present authors^[9].

SAMPLES AND MEASUREMENT METHOD

We investigated polycrystalline samples of the M structure ($SrFe_{12}O_{19}$, $PbFe_{12}O_{19}$ and W structure $BaNi_2Fe_{16}O_{27}-Ni_2W$, $BaMg_2Fe_{16}O_{27}-Mg_2W$, and also single-crystal $BaFe_{12}O_{19}$. The polycrystalline samples were prepared by the usual ceramic technology from iron oxide enriched with Fe^{57} to 87%. The single-crystal $BaFe_{12}O_{19}$ was grown by M. A. Balbashev by recrystallization of polycrystalline powder. The sample was cylindrical with 5 mm diameter and 13 mm length. The easy-magnetization axis (the hexagonal C axis) was perpendicular to the cylinder axis.

The measurements were performed with a spin-echo setup in the temperature range 4.2–300°K. At 4.2°K, the sample-holding coil, which was inductively coupled to the radio-frequency generator, was placed in a helium Dewar. In measurements in the range

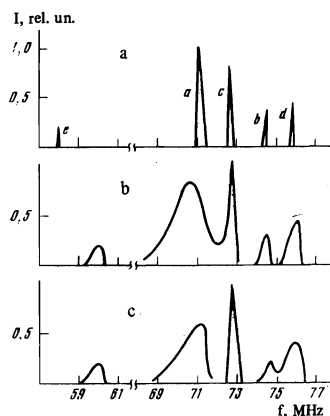


FIG. 1

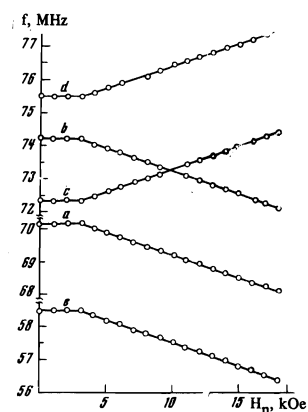


FIG. 2

FIG. 1. Fe^{57} echo-signal intensity vs. frequency at 4.2°K: a—single crystal $BaFe_{12}O_{19}$, b—polycrystalline $SrFe_{12}O_{19}$; c—polycrystalline $PbFe_{12}O_{19}$.

FIG. 2. Change of resonant frequencies of five sublattices in single-crystal $BaFeO_{19}$ vs. the magnetic field at $T = 77^\circ K$.

77–300°K, the usual scheme of blowing nitrogen vapor was used. The temperature was registered with a chromel-copel thermocouple. The resonant frequency, determined from the beats between the pulse carrier frequency and the signal from the G4-44 generator, was measured with a ChK 3-4A instrument. To obtain the necessary frequency resolution, radio-frequency pulses of duration not less than 20 sec were applied to the sample.

MEASUREMENT RESULTS

1. $MFe_{12}O_{19}$ with $M = Ba, Sr, and Pb$. Plots of the echo-signal intensity against the frequency at 4.2°K are given in Fig. 1 for $BaFe_{12}O_{19}$, $SrFe_{12}O_{19}$, and $PbFe_{12}O_{19}$. In $BaFe_{12}O_{19}$, the spectrum consists of five individual lines designated a, b, c, d, and e. We note that the line width in the single-crystal $BaFe_{12}O_{19}$ is approximately 60–80 kHz, which is much less than the line width in polycrystalline samples.^[9]

Figures 2 and 3 show plots of the resonant frequencies f against the magnitude and direction of the external magnetic field in $BaFe_{12}O_{19}$. In the measurements of the angular dependences in a field $H = 16$ kOe (Fig. 3), the sample was rotated about the cylinder

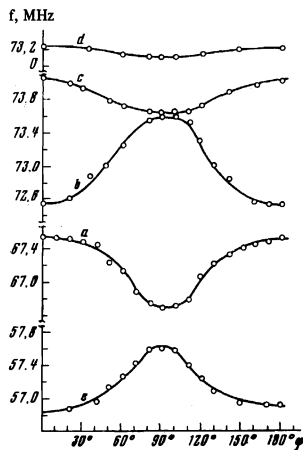


FIG. 3

FIG. 3. Angular dependence of the change of the resonant frequencies in single-crystal $\text{BaFe}_{12}\text{O}_{19}$ at $H = 16$ kOe and $T = 77^\circ\text{K}$.

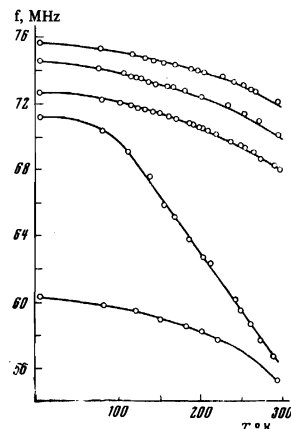


FIG. 4

FIG. 4. Temperature dependence of the change of the NMR resonant frequencies in $\text{SrFe}_{12}\text{O}_{19}$.

axis in such a way that the C axis could make an angle from 0 to 180° with the direction of the external magnetic field.

Figure 4 shows the temperature dependences of the resonant frequencies in the temperature range 4.2 – 300°K for the ferrite $\text{SrFe}_{12}\text{O}_{19}$. Analogous plots are observed also for $\text{PbFe}_{12}\text{O}_{19}$. Data on the temperature dependences of the resonant frequencies in $\text{BaFe}_{12}\text{O}_{19}$ were published earlier^[9]. Typical values of the intensity for the line a 4.2°K correspond to a signal/noise ratio 30. At room temperatures, this value decreases to 5–10. With increasing magnetic field, the intensity of the signal changes little. In addition to investigating the resonant frequencies and the intensity of the signal in $\text{BaFe}_{12}\text{O}_{19}$, we measured the longitudinal and transverse relaxation times T_1 and T_2 , which are listed in Table I. It should be pointed out that in the single crystal the values of the parameters T_1 and T_2 , as well as their temperature dependences, differ from the data obtained for polycrystalline samples^[9].

2. Ni_2W and Mg_2W . Figures 5 and 6 shows the NMR spectra and the temperature dependences of the resonant frequencies for Ni_2W and Mg_2W , respectively. In these samples, the signal intensity is several times weaker than in the hexaferrites of M structure. The characteristic values of the relaxation time at $T = 2^\circ\text{K}$ are $T_1 = 10$ msec and $T_2 = 5$ msec in the Mg_2W ferrite.

DISCUSSION OF RESULTS

The unit cells of a ferrite with structure M or W^[10] consist of alternating spinel blocks S, containing oxygen and iron ions, and hexagonal blocks R, containing Ba, Sr, or Pb ions in addition to the oxygen and iron ions. The M structure can be represented in the form of one S block and one R block, and the W structure in the form of two S blocks and one R block. The iron ions in such structures can occupy three types of sites: octahedral, tetrahedral, and sites having an environment consisting of five oxygen ions. The 12 iron M-

Table I. Longitudinal (T_1) and transverse (T_2) relaxation time in single-crystal $\text{BaFe}_{12}\text{O}_{19}$ at 4.2°K

	a	b	c	d	e
T_1 , msec	250	220	200	220	210
T_2 , msec	5	11	9	3	3

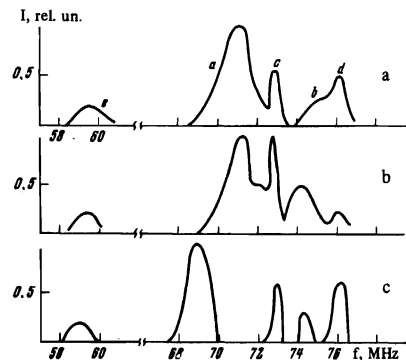


FIG. 5. Dependence of the amplitude of the echo signal on the frequency: a— Ni_2W at $T = 4.2^\circ\text{K}$ and $H = 0$; b— Mg_2W at $T = 4.2^\circ\text{K}$ and $H = 0$; c— Ni_2W at $T = 77^\circ\text{K}$ and $H = 10$ kOe.

Table II. Designation of the NMR lines in M-structure ferrites, type of oxygen environment, number of ions per formula unit, spin direction in the magnetic sublattices

Line	Position	Number of ions	Spin	Block
a	octahedral	6	\uparrow	S and R
b	octahedral	1	\downarrow	S
c	tetrahedral	2	\downarrow	S
d	octahedral	2	\downarrow	R
e	fivefold	1	\uparrow	R

structure ions make up five magnetic sublattices and are arranged as follows: six ions in octahedra (spin up), one ion in the fivefold oxygen environment (spin down), and two ions in octahedra (spin down). The identification of the NMR line with the iron ions corresponding to the different sublattices can be based on data on the line shifts as functions of the external magnetic field and of the relative intensity. This identification is given in Table II.

The NMR frequency is determined by the average value of the local field at the given temperature:

$$\omega_i = \gamma |\langle H_{loc,i} \rangle|, \quad (1)$$

$$|\langle H_{loc,i} \rangle| = |H_{hf} + H_{dip} + H_0|.$$

Here $H_{hf} = -A_0 M_i$ is the hyperfine field, H_0 is the hyperfine-interaction constant, M_i is the magnetization of the i -th sublattice per atom, H_{dip} is the dipole field, H_0 is the external magnetic field, and γ is the gyromagnetic ratio of the nuclei.

If the directions of H_{loc} and H_0 differ by a certain

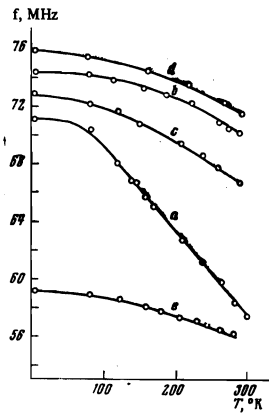


FIG. 6. Temperature dependence of the NMR resonance frequencies in Mg_2W .

Table III. Effective value of the gyromagnetic ratio of the Fe^{57} nuclei and angle of inclination of the magnetic moments to the C-axis direction of the five sublattices in single crystal $BaFe_{12}O_{19}$

	a	b	c	d	e
$\gamma_{eff}/2\pi$, Hz/Oe	135,6	135,2	138	135,1	137,8
α , deg	10 ± 4	11 ± 4	0	11 ± 5	0

angle φ , then, recognizing that $H_0 \ll H_{hf}$

$$f_i(H) = f_i(0) \pm \frac{\gamma}{2\pi} H_0 \cos \varphi_i + \frac{1}{2} \frac{\gamma}{2\pi} \frac{H_0^2}{H_{hf i}} \quad (2)$$

By measuring the dependence of the change of the resonant frequencies on the magnetic field (Fig. 2), we can determine $\gamma_{eff} = \gamma \cos \varphi_i$, where the gyromagnetic ratio for the Fe^{57} nuclei is $\gamma = 137.7$ Hz/Oe^[11]. The figures given in Table III, while close to this value, differ in the case of the sublattices a, b, and d from 137.7 Hz/Oe by an amount exceeding the measurement error. These discrepancies signify that the direction of the local field is not collinear with respect to the direction of the external magnetic field H_0 . We can point out several sources of non-collinearity of the hyperfine and external magnetic fields:

1. Insufficiently accurate orientation of the sample, so that $H_0 \neq C$.

In this case φ denotes the angle between H_0 and C. This reason cannot account for our results, for in this case all the NMR lines would have γ_{eff} of equal magnitude and not equal to γ . In addition, we can state that in our experiments the orientation of H_0 along the C axis is within not more than $2-3^\circ$, since the sample could be freely oriented along the magnetic field. The sample was freely placed in the coil before the start of the measurement.

2. The dipole fields of the surrounding ions and the tensor properties of the hyperfine-interaction constant.

If the constant A_0 is a tensor and none of the tensor axes coincides with the C axis, then the direction of the hyperfine field may not coincide with the Z axis even if the ion magnetization is directed along this axis. A similar result can be produced also by the dipole

fields from the surrounding magnetic ions. From the NMR data it is impossible to separate the contributions from the dipole fields and from the anisotropy of the constant A_0 . But there is no need for this, if an upper bound is estimated for the angle by which the local field can deviate from the magnetization direction. Let us find this estimate for the particular case of dipole interactions. The dipole field producing a moment μ located at a distance r from the nucleus is equal to

$$H_{dip} = \frac{3r(\mu r) - \mu r^2}{r^5} \quad (3)$$

Let the μ axis be directed along Z, and let r lie in the ZY plane. It is then easy to verify by direct calculation that the maximum field perpendicular to μ is $H = 3\mu Z/2r^3$. When the direction of μ changes relative to the Z axis (i.e., when μ rotates in the XY plane), the value of the field H_Z will change from $-\mu Z/r^3$ to $2\mu Z/r^3$, and the total swing will be $\Delta H_Z = -3\mu Z/r^3$. It follows therefore that by measuring the angular dependence for a local field we determine the quantity $\Delta H_Z = 3\mu Z/r^3$ and we can estimate the maximum values of the perpendicular component $3\mu Z/2r^3 = (\frac{1}{2})\Delta H_Z$. The angle between the local field and the direction of the magnetization is determined from the relation

$$\sin \varphi = \Delta H_Z / 2H_{loc} \quad (4)$$

We have investigated the angular dependences for a local field (see, for example, Fig. 3) at different orientations of the constant magnetic field relative to the C axis. According to our data, the largest swing of the angular dependences is $\Delta H_Z = 10$ kOe. According to Mössbauer-effect data^[2], this value is 14 kOe. Thus, even at the maximum field $(\frac{1}{2})\Delta H_Z = 7$ kOe, the angle is $\varphi = 0.013$ rad $\approx 0.7^\circ$.

3. The last possible explanation of the values of φ given in Table III is the non-collinearity of the sublattice magnetization.

We note that γ_{eff} is determined with accuracy $5-6\%$, a value governed by the inaccuracy of the orientation of the sample and by the inaccuracy of the registration of the resonant frequency as a result of instrumental errors and the natural line width. The accuracy with which the magnetic field is measured is $\leq 1\%$. The magnet was calibrated with the IMI-2 instrument and was additionally corrected by measuring the NMR in a $Y_3Fe_5O_{12}$ sample as a function of the field. It is known from Robert's paper^[12] that the magnetic moments of the iron ions in $Y_2Fe_5O_{12}$ are strictly antiparallel.

In accordance with the data given in Table III, we can assume the existence of a small non-collinearity in the arrangement of the sublattice moments. Generally speaking, non-collinearity was observed in hexagonal ferrites of complex composition^[13]. This, however, is the first indication of non-collinearity in $BaFe_{12}O_{19}$. It is of interest to compare the results with the published experimental data on magnetic measurements of the total saturation magnetization. It is easy to verify that the proposed non-collinearity should make the resultant summary magnetic moment smaller than the nominal value by 5%. According to data by Henry^[14] and Casimir^[15] this value fluctuates between 19.6 and 20.4 μ_B and the maximum value of the mag-

netization per formula unit in the case of collinear arrangement should be $20 \mu_B$.

Thus, magnetic measurements at low temperatures do not give any grounds for assuming large deviation angles from collinearity. The assumption of a non-collinearity of several degrees, however, does not contradict the magnetic-measurement data. Neutron-diffraction investigation^[16] revealed no non-collinearity within the limits of the measurement errors. The figures obtained in our paper are practically at the limits of accuracy of magnetic measurements, neutron diffraction, and NMR. It is therefore not surprising that the nonparallel disposition of the magnetic moments in $\text{BaFe}_{12}\text{O}_{19}$ was not observed previously. In our study, the angles are determined with a rather large error, and the data indicate mainly that if non-collinearity does exist, it does not exceed the values given in the table, and the magnetic moments of the $\text{BaFe}_{12}\text{O}_{19}$ sublattices should form a cone in such a way that the total magnetization is directed along the C axis.

TEMPERATURE DEPENDENCES OF THE SUBLATTICE MAGNETIZATIONS

The temperature dependences of the sublattice magnetizations can be determined from the temperature dependences of the resonant NMR frequencies (formula (3)). The temperature dependences of the resonant frequencies of all the investigated ferrites of M and W structure have the same character. This is due primarily to the small difference between the Curie points. On the basis of the experimental dependences of the sublattice magnetizations, we can calculate the parameters of the principal exchange interactions by using the molecular-field theory. The calculations are similar to the earlier ones^[9].

We represent the sublattice magnetization in the following form:

$$\begin{aligned} \frac{M_a(T)}{M_a(0)} &= B_S \left[\frac{2S[Z_{aa}J_{aa}M_a(T) + Z_{ca}J_{ac}M_c(T)]}{g\mu_B kT} \right], \\ \frac{M_b(T)}{M_b(0)} &= B_S \left[\frac{2SZ_{cb}J_{bc}M_c(T)}{g\mu_B kT} \right], \\ \frac{M_c(T)}{M_c(0)} &= B_S \left[\frac{2S[Z_{ac}J_{ca}M_a(T) + Z_{oc}J_{cb}M_b(T)]}{g\mu_B kT} \right], \\ \frac{M_d(T)}{M_d(0)} &= B_S \left[\frac{2S[Z_{ad}J_{da}M_a(T) + Z_{ed}J_{ed}M_e(T)]}{g\mu_B kT} \right], \\ \frac{M_e(T)}{M_e(0)} &= B_S \left[\frac{2SZ_{ae}J_{ea}M_a(T)}{g\mu_B kT} \right], \end{aligned} \quad (5)$$

where B is the Brillouin function, k is Boltzmann's constant, S is the spin of the Fe^{2+} ion, $g = 2$, and Z_{ij} is the number of nearest neighbors of the sublattice j from the sublattice i. The coefficients Z_{ij} are listed

Table IV. Values of the coefficients

	a	b	c	d	e
a	0	0	3	2	0
b	0	0	6	0	0
c	9	3	0	0	0
d	6	0	0	0	3
e	6	0	0	6	0

Table V. Exchange integrals J_{bc} , J_{ed} , J_{ac} , and J_{ad}

	$\frac{J_{bc}}{k^\circ\text{K}}$	$\frac{J_{ed}}{k^\circ\text{K}}$	$\frac{J_{ac}}{k^\circ\text{K}}$	$\frac{J_{ad}}{k^\circ\text{K}}$
$\text{BaFe}_{12}\text{O}_{19}$	24	19	9	18
$\text{SrFe}_{12}\text{O}_{19}$	21	18	10	16
$\text{PbFe}_{12}\text{O}_{19}$	19	18	10	16

in Table IV. (We note that in^[9] Z was chosen equal to the number of ions in the sublattice.) The calculations were performed with a "Promin" computer by selecting the optimal values of the exchange integrals calculated at different temperatures from the condition of the best fit of the theoretical and experimental plots of the sublattice magnetizations (deviation not larger than 10%).

Table V lists the values of the exchange integrals per exchange bond. The exchange integrals for $\text{BaFe}_{12}\text{O}_{19}$ were taken from^[9] with allowance for the coefficients Z_{ij} of Table IV. The data on the temperature dependences of the sublattice magnetizations enable us to determine the temperature dependence of the total saturation magnetization per formula unit. In the case of a collinear arrangement of the magnetic moments

$$M(T) = \sum_{i=1}^5 C_i M_i, \quad (6)$$

where M is the total magnetization, C_i is a coefficient that depends on the number of ions in the sublattice and on the direction of their spins.

We note that a similar method of determining the total magnetization has the following advantages in comparison with the usual magnetization measurements methods: 1) NMR measurements are usually performed in a zero magnetic field, whereas strong magnetic fields (more than 20 kOe), which are needed to saturate the sample, can change the magnetic structure in the measurements of the total magnetization. 2) In measurements of the macroscopic magnetization, the magnetic impurities and extraneous phases can lead to inaccuracies in the determination of the magnetic moment of the sample. NMR is not sensitive to impurities and to extraneous phases.

From a comparison of the temperature dependence of the total magnetization, obtained on the basis of NMR data and formula (6), with the measurements of the total saturation magnetization, we were able to determine the most probable cation distribution of the Mg ions in the Mg_2W . In the calculations based on formula (6), we considered in succession the following possible substitutions of the iron ions: 1) in position a, 2) in position b, 3) in position d, 4) statistical substitution in the octahedral positions. We did not consider variants of substitution in the fivefold coordination e and in the tetrahedra c, for in those cases the summary magnetization should increase in comparison with Fe_2W , whereas it actually is lower. The best agreement between the calculated (from the NMR data) and observed total magnetization is obtained if it is assumed that the Mg^{2+} ions replace the iron ions in octahedral position b (see Fig. 7).

The authors thank G. A. Smolenskiĭ for interest in

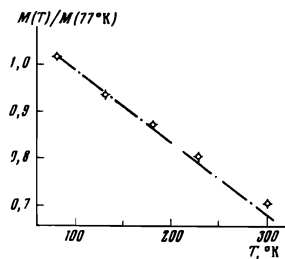


FIG. 7. Temperature dependence of the magnetization of Mg_2W . Dark circles—results of measurement of the total magnetization. Solid line—calculation by formula (6) using NMR data under the assumption that the Mg ions replace the iron ions in the octahedral position b.

the work and A. M. Bolbashov for preparing the $\text{BaFe}_{12}\text{O}_{19}$ single crystal.

¹J. J. Loef and J. M. Franssen, Phys. Lett., 7, 225 (1963).

²J. J. Loef and A. Groenou, Proc. of the Intern. Conf. on Magnetism, Nottingham, 1964, The Inst. of Phys. and Phys. Soc., London, 1965.

³V. Zinn, Zs. Angew. Phys., 17, 147 (1964).

⁴J. S. Wierningen and J. G. Rinssen, Zs. Angew. Phys., 21, 69 (1966).

⁵J. S. Wierningen, Phillips. Tech. Rev., 28, 33 (1967).

⁶G. Albanes, G. Asti, and P. Batti, Nuovo Cim., 54B, 339 (1968).

⁷T. A. Khimich, V. F. Belov, M. N. Shipko, and E. V. Kornev, Zh. Eksp. Teor. Fiz. 57, 395 (1969) [Sov. Phys.-JETP 30, 217 (1970)].

⁸R. L. Streever, Phys. Rev., 186, 285 (1969).

⁹M. P. Petrov and A. V. Kunevich, Izv. AN SSSR 35, 1090 (1971).

¹⁰J. Smit and H. P. J. Wijn, Ferrites, Wiley, 1959.

¹¹G. W. Ludwig and H. H. Woodburi, Phys. Rev. 117, 1286 (1960).

¹²C. Robert and C. R. Paris, 252, 1442 (1961).

¹³M. I. Namtashvili, O. P. Oleshko-Ozhevskii, and I. I. Yamzin, Fiz. Tverd. Tela 13, 2543 (1971) [Sov. Phys.-Solid State 13, 2137 (1972)].

¹⁴W. E. Henry, Phys. Rev., 112, 326 (1958).

¹⁵H. Casimir, J. Phys. Rad., 20, 360 (1959).

¹⁶O. P. Oleshko-Ozhevskii, Kristallografiya 14, 447 (1969) [Sov. Phys.-Crystallogr. 14, 367 (1969)].

Translated by J. G. Adashko
245